Model of Magnetic Anisotropy of Non-Oriented Steel Sheets for Finite Element Method

Floran Martin[1], Deepak Singh[1], Paavo Rasilo[1,2], Anouar Belahcen[1], and Antero Arkkio[1]

[1]Aalto University, Dept. of Electrical Engineering and Automation, P.O. Box 13000, FI-00076 Espoo, Finland
[2]Tampere University of Technology, Dept. of Electrical Engineering, P.O. Box 692, FI-33101 Tampere, Finland

Even non-oriented steel sheets present a magnetic anisotropic behavior. From rotational flux density measurements at 5 Hz, the model of magnetic anisotropy is derived from two surface Basis-cubic splines with the boundary conditions matching with ferromagnetic theory. Furthermore, the investigation of the magnetic anisotropy shows that the $\boldsymbol{H}(\boldsymbol{B})$ characteristic is not strictly monotonous due to the angle difference between the field and the flux density. Hence, standard non-linear solvers would either diverge or converge towards the closest local minimum. Thus, we propose two different specific solvers: a combined Particle Swarm Optimization with a relaxed Newton-Raphson and a Modified Newton Method.

***Index Terms*—Magnetic anisotropy, modified Newton method, Newton Raphson, non-oriented steel sheet, particle swarm optimization, surface basis-cubic spline**

I. Introduction

NON-ORIENTED (NO) electrical steel sheets are usually composed of iron doped with silicon. Although their manufacturing process tends to confer isotropic properties [1], [2], magnetic anisotropy has been always observed and recently investigated [3], [4], [5].

Models of magnetic anisotropy derive from different formulations regarding to the target application. Since the magnetic anisotropy infers a dependence of reluctivity on both amplitude and direction of the applied flux density, its model can be developed by interpolating between two adjacent measured B-H curves [6]. Under rotational applied flux density, Enokizono and Soda [7] develop a Galerkins formulation based on the decomposition of the magnetic reluctivity into an isotropic part and an anisotropic part. Both components of reluctivity are interpolated and implemented into their numerical method.

Based on energy/coenergy density principle [8], Péra et al [9] expand a phenomenological model on grain oriented sheets which needs only the rolling (RD) and the transverse (TD) direction given by manufacturers. However, the four magnetization modes introduced by Néel [10] are not fully described by this phenomenological approach, so data in more directions are needed to characterize these sheets completely [5], [11]. Thus, Higuchi et al. [5] model the magnetic energy density for NO sheets with Fourier series for alternating flux with 7 different directions. In order to reduce the computational effort required by the Fourier series, Martin et al [12] developed an analytical model of the energy density whith three functional parameters which are based on Gumbel distribution. However, reducing the computational effort with analytical models is usually involving a lower accuracy.

In this paper, we propose to model the polar components of the magnetic field with two surface Basis-splines depending on the polar components of the magnetic flux density. Hence the proposed model should provide a relatively good accuracy among other approaches. From rotational measurements, the magnetic losses are first removed and then an extrapolation of the magnetic loci is performed. Since the phase theory presents more than a single easy direction, the non-linear solver should be able to avoid some local minima. In this paper, we propose two solvers : the first one is a combination of a Particle Swarm Optimization (PSO) [13] with a relaxed Newton Rapshon method. The second one is a Modified Newton Method derived from a continuous Newton method [14].

II. Model of magnetic anisotropy with 2 surface B-cubic splines

The magnetic measurements are first extrapolated in order to extend the definition set for the non-linear solver. Then, the measurements of the polar components of the magnetic field (H, ϕ_h) are interpolated as a function of the polar components of the magnetic flux density (B, ϕ_b) with two surface B-cubic splines.

A. Extrapolation of B-H loci

Measurements have been carried out at 5 Hz with a sampling rate of 10 kHz in a cross shape NO sheet. The rotating magnetic flux density presents 16 amplitudes from 0.1 T to 1.6 T with a step of 0.1 T and an accuracy of 0.5 %. For extracting the anisotropy, the magnetic losses are removed by canceling the phase shift between both fundamental

Manuscript received April 1, 2015; revised May 15, 2015 and June 1, 2015; accepted July 1, 2015. Date of publication July 10, 2015; date of current version July 31, 2015. (Dates will be inserted by IEEE; "published" is the date the accepted preprint is posted on IEEE Xplore®; "current version" is the date the typeset version is posted on Xplore®). Corresponding author: F. Martin (e-mail: floran.martin@aalto.fi). If some authors contributed equally, write here, "F. A. Author and S. B. Author contributed equally." IEEE TRANSACTIONS ON MAGNETICS discourages courtesy authorship; please use the Acknowledgment section to thank your colleagues for routine contributions.

Color versions of one or more of the figures in this paper are available online at http://ieeexplore.ieee.org.

Digital Object Identifier (inserted by IEEE).

components of magnetic flux density and magnetic field [12].

The extrapolation of the magnetic anisotropy is performed by assuming that the amplitude of the magnetization can be modeled by the solution of a second order differential equation with a step source. Only the over-damped case is considered in order to preserve a strictly monotonous B-H curve. The amplitude B of the magnetic flux density can be interpolated by:

$$\begin{aligned} B &= M_s \left[k_1 \exp\left(-\omega_0 \left[\xi + \sqrt{\xi^2-1}\right] H\right)\right. \\ &\quad \left. + \exp\left(-\omega_0 \left[\xi - \sqrt{\xi^2-1}\right] H\right)\right] + \mu H \end{aligned} \tag{1}$$

where M_s, k_1, ω_0, ξ and μ are the model parameters.They are fitted for every measured angle of the magnetic flux density ϕ_b.

In Fig. 1a and Fig. 1c, the proposed analytical extrapolation can reproduce the trend of the $B-H$ curve with a relatively good accuracy the non-linear magnetic curve.

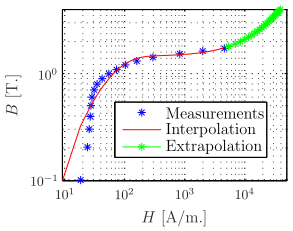

(a) Amplitude of $\boldsymbol{H}$ at 0°

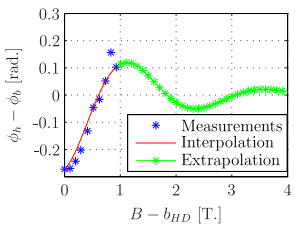

(b) Angle shift $\phi_h - \phi_b$ at 0°

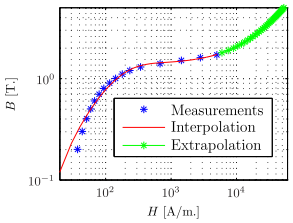

(c) Amplitude of $\boldsymbol{H}$ at 55°

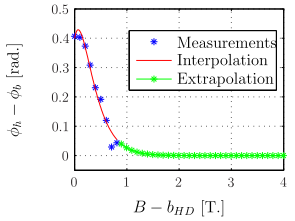

(d) Angle shift $\phi_h - \phi_b$ at 55°

Fig. 1. Extrapolation of the magnetic field components with respect to the amplitude of the magnetic flux density when the flux density angle is oriented toward the rolling and the hard direction.

The extrapolation of the polar angle of the magnetic field is carried out with a similar reasoning. The angle difference between the magnetic field and the flux density can be extrapolated by considering a solution of a second order differential equation with a non-nil initial condition and without source. This non-nil initial condition matches with the maximum angle difference $\Delta\phi_m(b_{HD})$. Depending on the direction of the magnetic flux density, this angle difference can present either the same sign as $\Delta\phi_m(b_{HD})$ (over-damped case) or some oscillations (under-damped case). Thus, the angle difference $\Delta\phi = \phi_h - \phi_b$ can be modeled as a function of the amplitude of the magnetic flux density by:

- Over-damped case:

$$\begin{aligned} \Delta\phi &= \Delta\phi_m \left[\tilde{k_1} \exp\left(-\tilde{\omega_0}\left[\tilde{\xi} + \sqrt{\tilde{\xi}^2-1}\right] B\right)\right. \\ &\quad \left. + \exp\left(-\tilde{\omega_0}\left[\tilde{\xi} - \sqrt{\tilde{\xi}^2-1}\right] B\right)\right] \end{aligned} \tag{2}$$

- Under-damped case:

$$\Delta\phi = \Delta\phi_m \exp\left(-\tilde{\omega_0}\tilde{\xi}B\right) \cos\left(\tilde{\omega_0}\sqrt{1-\tilde{\xi}^2}\, B + \tilde{\varphi}\right) \tag{3}$$

where $\tilde{k_1}$, $\tilde{\omega_0}$, $\tilde{\xi}$ and $\tilde{\varphi}$ are parameters of the models. They are also fitted for every measured angle of the magnetic flux density ϕ_b. In Fig. 1b and Fig. 1d, the proposed analytical extrapolation can reproduce with a relatively good accuracy the angle difference between the field and the flux density.

B. Surface spline models for polar components of the magnetic field and flux density

The uniformly distributed polar components of the magnetic flux density are sorted with ascending order. Their indices are denoted r and h respectively for B and ϕ_b. For $B_r \leq B \leq B_{r+1}$ and $\phi_{b_h} \leq \phi_b \leq \phi_{b_{h+1}}$, a polar component of the magnetic field S can be modeled with a parametric surface B-cubic spline, expressed by [15], [16]:

$$S(u,v) = \frac{1}{36}\begin{bmatrix} u^3 & u^2 & u & 1 \end{bmatrix} \mathbf{C}\mathbf{Q}\mathbf{C}^T \begin{bmatrix} v^3 \\ v^2 \\ v \\ 1 \end{bmatrix} \tag{4}$$

with

$$\mathbf{C} = \begin{bmatrix} -1 & 3 & -3 & 1 \\ 3 & -6 & 3 & 0 \\ -3 & 0 & 3 & 0 \\ 1 & 4 & 1 & 0 \end{bmatrix} \tag{5}$$

$$\mathbf{Q} = \begin{bmatrix} Q_{r,h} & Q_{r,h+1} & Q_{r,h+2} & Q_{r,h+3} \\ Q_{r+1,h} & Q_{r+1,h+1} & Q_{r+1,h+2} & Q_{r+1,h+3} \\ Q_{r+2,h} & Q_{r+2,h+1} & Q_{r+2,h+2} & Q_{r+2,h+3} \\ Q_{r+3,h} & Q_{r+3,h+1} & Q_{r+3,h+2} & Q_{r+3,h+3} \end{bmatrix} \tag{6}$$

where $\mathbf{Q}$ contains the control points and $\mathbf{C}$ is derived from [16]. u and v are local coordinates of the amplitude and the angle of the flux density respectively $(u,\, v) \in [0,\, 1]^2$.

For n different amplitudes of $\boldsymbol{B}$ and m different angles of $\boldsymbol{B}$, the surface B-cubic spline interpolation requires $(n{+}2)(m{+}2)$ unknown control points. The interpolation of a polar component of $\boldsymbol{H}$, composed of the terms $P_{n(h-1)+r}$, is ensured by the following set of nm equations:

$$P_{n(h-1)+r} = S(0,0) \tag{7}$$

The remaining $2n + 2m + 4$ equations are determined by the boundary conditions which depends on the problem. A set

of $2n$ equations is determined in order to ensure a periodic condition corresponding to $\phi_b = 0$ and $\phi_b = 2\pi$.

$$\left.\frac{\partial S(0,0)}{\partial v}\right|_{r,h=1} = \left.\frac{\partial S(0,1)}{\partial v}\right|_{r,h=m-1}$$
$$\left.\frac{\partial^2 S(0,0)}{\partial v^2}\right|_{r,h=1} = \left.\frac{\partial^2 S(0,1)}{\partial v^2}\right|_{r,h=m-1} \quad (8)$$

For the interpolation of ϕ_h, the periodic condition is still holding so a similar set of $2m$ equations is considered. Concerning the interpolation of H, some inflection points exist at 0 T for any angle ϕ_b. Moreover, the material is supposed fully saturated at 2.7 T. This value can also be chosen higher since the extrapolation can provide some data for higher value of B. Thus, it results the set of $2m$ equations:

$$\left.\frac{\partial H(1,0)}{\partial u}\right|_{r=n-1,h} = \nu_0; \qquad \left.\frac{\partial^2 H(0,0)}{\partial u^2}\right|_{r=1,h=1} = 0 \quad (9)$$

The remaining 4 equations for both components of $\boldsymbol{H}$ respect the symmetry along ϕ_b between the 4 boundary corner data points and the inner data points by imposing 4 "not-a-knot" conditions. Finally the required control points are determined by solving this system of $(n{+}2)(m{+}2)$ equations.

C. Analysis of the proposed model

In Fig. 2a, the accuracy of the proposed interpolation can be appreciated. Even if the interpolation of both surface spline should pass through every data points, a maximum relative error of -0.03% is reached for the amplitude of $\boldsymbol{H}$ at the corner (2.7 T, 2π rad). For the interpolation of the angle of $\boldsymbol{H}$, the maximum relative error is 4% at the corner (0 T, 0 rad) but every corner presents some smaller errors.

Moreover, the model $\boldsymbol{H}(\boldsymbol{B})$ shows some local minima since the Jacobian $\partial\boldsymbol{H}/\partial\boldsymbol{B}$ is not always positive definite. This phenomenon appears mainly when the angle of $\boldsymbol{H}$ is almost constant while the angle of $\boldsymbol{B}$ is linearly increasing (Fig. 2b).

III. Solvers for the Proposed Non-Linear Anisotropic Magnetic Model

To ensure the convergence toward the global minimum, we propose two solvers based on the Newton method. A classical Newton-Raphson method presents a fast convergence but it can only track the closest minimum. In spite of a slow convergence, evolutionary algorithms present good performance to track the global minimum. In order to benefit these two advantages, the first solver is a combination of a Particle Swarm Optimization (PSO) [13] with a relaxed Newton method. The second solver is a Modified Newton Method derived from a continuous Newton method [14].

A. Combined PSO with a Newton-Raphson method

This main algorithm is the standard Particle Swarm Optimization described in [13]. The Newton-Raphson with an adaptive relaxation factor is launched on the particle holding the maximum residual only if this residual $\boldsymbol{R}$ remains constant after 50 iterations. The iterative relaxed Newton-Raphson is modeled by:

$$\boldsymbol{x}_{k+1} = \boldsymbol{x}_k - \alpha \left[\mathbf{J}(\boldsymbol{x}_k)\right]^{-1} \boldsymbol{R}(\boldsymbol{x}_k) \quad (10)$$

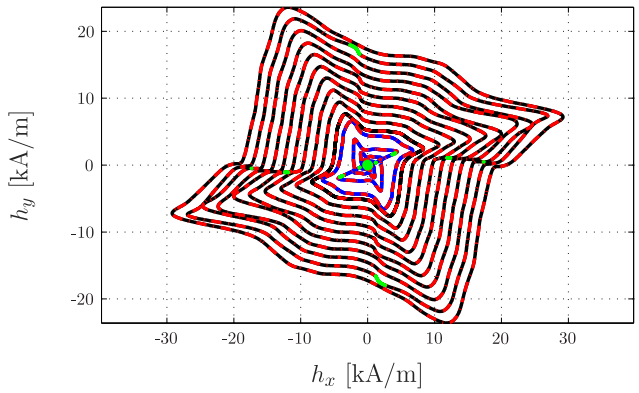

(a) $\boldsymbol{H}$ loci

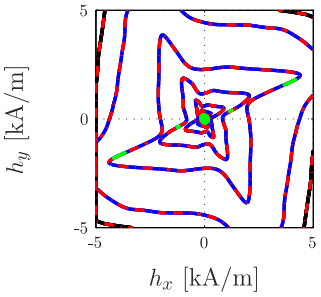

(b) Zoom in the measurements range

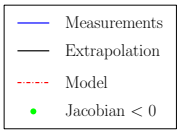

(c) Legend

Fig. 2. Measurements, interpolation and extrapolation of $\boldsymbol{H}$ loci . The axis denoted h_x corresponds to the rolling direction.

where $\boldsymbol{x}$ and $\boldsymbol{R}$ are two explicit functions of the magnetic flux density $\boldsymbol{B}$ and the magnetic field $\boldsymbol{H}$ respectively, $\mathbf{J}$ is the Jacobian given by $\mathbf{J} = \partial\boldsymbol{R}/\partial\boldsymbol{x}$ and α is the relaxation factor. In order to ensure the convergence toward the closest minimum, this relaxation factor is determined so that it minimizes the residual.

B. Modified Newton Method

The Modified Newton Method is derived from a continuous Newton method [14]. Thus, its continuous form consists of solving a set of first order Ordinary Differential Equations (ODEs) given by:

$$\frac{d\boldsymbol{x}}{dt} = -\left[\mathbf{J}(\boldsymbol{x})\right]^{-1} \boldsymbol{R}(\boldsymbol{x}) \quad \text{with} \quad \boldsymbol{x}(0) = \boldsymbol{x}_0 \quad (11)$$

where t is a fictitious variable ($0 \leq t < +\infty$).
After carrying out the variable transformation $s = 1 - \exp(-t)$, the continuous Newton method becomes for $0 \leq s < 1$:

$$(1-s)\mathbf{J}(\boldsymbol{x})\frac{d\boldsymbol{x}}{ds} + \boldsymbol{R}(\boldsymbol{x}) = 0 \quad \text{with} \quad \boldsymbol{x}(0) = \boldsymbol{x}_0 \quad (12)$$

This set of ODEs can be solved with a backward Euler method by uniformly discretizing s into $\tilde{m}$ sub-intervals:

$$(1-s_i)\mathbf{J}(\boldsymbol{x}_i)\tilde{m}\left[\boldsymbol{x}_i - \boldsymbol{x}_{i-1}\right] + \boldsymbol{R}(\boldsymbol{x}_i) = 0 \quad (13)$$

Besides, it can be shown that the resolution of a system of non-linear equations $\boldsymbol{R}(\boldsymbol{x}) = 0$ can be performed by solving a nonautonomous first order ODEs given by:

$$\frac{d\boldsymbol{x}}{d\tau} = -\frac{\nu}{1+\tau}\boldsymbol{R}(\boldsymbol{x}) \quad \text{with} \quad \boldsymbol{x}(0) = \boldsymbol{x}_0 \quad (14)$$

where the roots of the residual are the fixed points of this equation and τ is a fictitious time variable.

Since (13) depends strongly on its initial condition, it would converge toward the closest local minimum. In order to overcome this difficulty, this set of equations can be solved with the continuous fixed point method given in (14). Finally, the system of ODEs becomes :

$$\frac{d\boldsymbol{x_i}}{d\tau} = -\frac{\nu}{1+\tau}\left[(1-s_i)\mathbf{J}(\boldsymbol{x}_i)\tilde{m}\left[\boldsymbol{x}_i - \boldsymbol{x}_{i-1}\right] + \boldsymbol{R}(\boldsymbol{x}_i)\right]$$
$$\boldsymbol{x}(0) = \boldsymbol{x}_0 \tag{15}$$

This set of ODEs is solved by a Runge-Kutta method of order 4 with a constant time step h_t.

C. Comparison of the proposed solvers

The two different solvers are tested by solving a set of non linear equations $\boldsymbol{H}(\boldsymbol{B}) - \boldsymbol{H}_{\text{ref}} = 0$, where $\boldsymbol{H}_{\text{ref}}$ is composed of 1 000 random magnetic field components belonging to the measurements range. The combined PSO with a Newton-Raphson method is composed of 20 particles. The parameters of Modified Newton Method are $\boldsymbol{x}_0 = \mathbf{0}$, $\tilde{m} = 8$, $\nu = 400$ and $h_t = 1,2.10^{-7}$. In Fig. 3, both proposed solvers converge. The proposed improvement of the PSO significantly decrease the number of iteration to reach the global minimum. The improvement only appears when the PSO already converges near the global minimum. Although, this solver reaches an acceptable tolerance with few hundreds iterations less than the Modified Newton Method. it requires more computational effort than the latter, since at every iteration the residual is evaluated 5 times more than the Modified Newton Method.

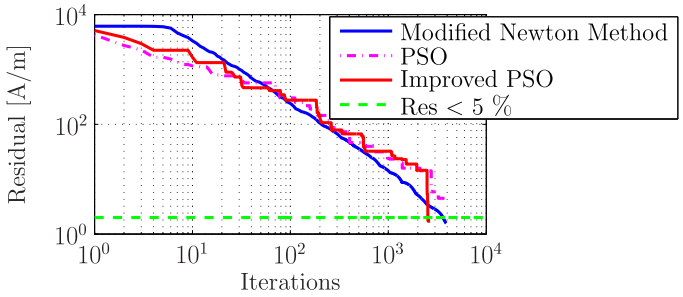

Fig. 3. Evolution of the residual of the proposed solvers

IV. Conclusion

The magnetic anisotropy of NO steel sheet is modeled with a relatively good accuracy by developing two surface B-cubic splines $H(B, \phi_b)$ and $\phi_h(B, \phi_b)$. Furthermore, the analysis of this magnetic property shows that the $\boldsymbol{H}(\boldsymbol{B})$ characteristic is not strictly monotonous, mainly due to the angle difference between the field and the flux density. Hence, standard numerical solvers would either diverge or converge towards the nearest local minimum. Finally, two specific solvers are proposed: a combined Particle Swarm Optimization with a Newton-Raphson and a Modified Newton Method. The former converges with the minimum number of iterations and the latter presents the minimum computational effort. In future work, the ferromagnetic theory should be able to analyze the source of the non strictly monotonous $\boldsymbol{H}(\boldsymbol{B})$ characteristic. Hence, the manufacturing process of NO steel sheet could be improved by diminishing the effect of this source. Moreover, the non-linear anisotropic model can be implemented into finite element analysis in order to investigate its effect on the specification of electrotechnical applications. Furthermore, the model could be extended in order to consider the anisotropic hysteretic behavior. For instance, the anisotropic splines could be implemented as the anhysteretic curves M_{an} in the Jiles-Atherton model.

Acknowledgment

The research leading to these results has received funding from the European Research Council under the European Union's Seventh Framework Programme (FP7/2007-2013) / ERC grant agreement n°339380. We also acknowledge the funding support of Academy of Finland.

References

[1] A. Kedous-Lebouc, *Matériaux magnétiques en génie électrique 1*. Lavoisier, 2006.
[2] P. Rasilo, E. Dlala, K. Fonteyn, J. Pippuri, A. Belahcen, and A. Arkkio, "Model of laminated ferromagnetic cores for loss prediction in electrical machines," *Electric Power Applications, IET*, vol. 5, pp. 580–588, August 2011.
[3] K. Chwastek, "Anisotropic properties of non-oriented steel sheets," *Electric Power Applications, IET*, vol. 7, pp. 575–579, Aug 2013.
[4] P. Handgruber, A. Stermecki, O. Biro, V. Gorican, E. Dlala, and G. Ofner, "Anisotropic generalization of vector preisach hysteresis models for nonoriented steels," *IEEE Trans. Magn.*, vol. 51, pp. 1–4, March 2015.
[5] S. Higuchi, Y. Takahashi, T. Tokumasu, and K. Fujiwara, "Comparison between modeling methods of 2-d magnetic properties in magnetic field analysis of synchronous machines," *IEEE Trans. Magn.*, vol. 50, no. 2, pp. 373–376, 2014.
[6] G. Shirkoohi and J. Liu, "A finite element method for modelling of anisotropic grain-oriented steels," *IEEE Trans. Magn.*, vol. 30, no. 2, pp. 1078–1080, 1994.
[7] M. Enokizono and N. Soda, "Magnetic field analysis by finite element method using effective anisotropic field," *IEEE Trans. Magn.*, vol. 31, no. 3, pp. 1793–1796, 1995.
[8] P. P. Silvester and R. P. Gupta, "Effective computational models for anisotropic soft b-h curves," *IEEE Trans. Magn.*, vol. 27, no. 5, pp. 3804–3807, 1991.
[9] T. Péra, F. Ossart, and T. Waeckerle, "Field computation in non linear anisotropic sheets using coenergy model," *IEEE Trans. Magn.*, vol. 29, no. 6, pp. 2425–2427, 1993.
[10] L. Néel, "Les lois de l'aimantation et de la subdivision en domaines élémentaires d'un monocristal de fer," *J. Phys. et Radium*, vol. 5, no. 11, pp. 241–251, 1944.
[11] G. Meunier, *The Finite Element Method for Electromagnetic Modeling*. Wiley-ISTE, 2008.
[12] F. Martin, D. Singh, A. Belahcen, P. Rasilo, A. Haavisto, and A. Arkkio, "Analytical model for magnetic anisotropy of non-oriented steel sheets," *COMPEL*, vol. 34, no. 5, pp. 1475–1488, 2015.
[13] R. Eberhart and J. Kennedy, "A new optimizer using particle swarm theory," in *Proceedings of the Sixth International Symposium on Micro Machine and Human Science*, pp. 39–43, 1995.
[14] S. Alturi, C. Liu, and C. Kuo, "A modified newton method for solving non-linear algebraic equations," *Journal of Marine Science and Technology*, vol. 17, no. 3, pp. 238–247, 2009.
[15] A. Valdescault, A. Batailly, and S. Jones, "Interpolation et approximation de données à l'aide de courbes et surfaces paramétriques de type b-splines," tech. rep., Université McGill - Montréal, 2012.
[16] C. De Boor, "On calculating with b-splines," *Journal of Approximation Theory*, vol. 6, pp. 50–62, 1972.